IARJSET ISSN (O) 2393-8021, ISSN (P) 2394-1588

International Advanced Research Journal in Science, Engineering and Technology

Impact Factor 7.105 ⁜ Vol. 9, Issue 2, February 2022

DOI: 10.17148/IARJSET.2022.9285

Structural and Spectroscopic studies of Europium doped Barium Titanate via solution combustion method

M.Dhanalakshmi[1*], Rajeshree Patwari D.[2]

[1,2]Nrupathunga university (Formerly Govt. Science College), Bengaluru-01, India

Abstract: The novel Eu^{3+} doped $BaTiO_3$ nanophosphors were synthesized by green combustion route using self-sacrificial Aloe Vera gel as a biofuel. The X-ray diffraction results showed the high purity with tetragonal crystal structure of $BaTiO_3$. From diffuse reflectance spectra, the energy gap of the prepared samples was estimated to be ~3.29-3.35 eV. Scanning electron microscopy results indicate various types of nano/microstructures which are highly dependent on concentration of Aloe Vera gel. The Eu^{3+} doped $BaTiO_3$ nanophosphor under UV light displays the characteristic red emission peaks corresponding to the $^5D_0 \rightarrow {}^7F_J$ transitions of Eu^{3+} ions. Concentration quenching phenomenon was discussed based on energy transfer, electron–phonon coupling and ion–ion interaction. Judd–Ofelt intensity parameters were calculated by using the Photo luminescence emission spectra. The emission colour of the nanophosphors was tuned from pale red to pure red region by varying the concentration of Eu^{3+} in the $BaTiO_3$ host. The prepared sample exhibit high color purity of ~ 92% and correlated color temperature was in the range ~ 2710-2115 K. The results indicate that the prepared phosphor was quite useful as warm and high purity red emission for solid state lighting applications.

Keywords: Nanophosphor, Photoluminescence, CIE, Solution combustion, Warm light

1. INTRODUCTION

In the recent years, research on phosphor converted LED's have attracted extensively due to energy saving, high efficiency, eco-friendly nature and longer lifetime advantages [1]. Sources like incandescent and fluorescent lamps were lower luminous efficacy lighting sources due to very poor sensitive to human eyes [2]. To overcome from these problems, rare earth doped titanates were drawn the attention for their unique applications in optical telecommunication, lasers, diagnostics, sensors, biological labels and luminescence [3]. It shows excellent dielectric properties in lead free devices, such as multilayer capacitors, thermistors, electro-optical devices and electromechanical devices. Barium titanate with perovskite structure has been attracting extensive attention for its excellent dielectric properties in lead free devices, such as multilayer capacitors, thermistors, electro optical devices and electromechanical devices [4-6].

Synthesis of nanomaterials by using green extracts are emerging trend to achieve the need of environmental benevolent technologies. Green synthesis is a versatile, easy to handle, cost effective and eco-friendly method. The use of biological entities for synthesis of nanomaterials found to have a probe over toxic chemicals and has gained substantial interest in the field of nanomaterials. Among the various natural products, phytochemicals have been promising as important natural resources for the synthesis of metal oxide nanoparticles. In the present work, Aloe Vera (A.V.) plant extract was used as a fuel to obtain $BaTiO_3$:Eu^{3+} nanophosphor by green synthesis route. A.V. belongs to the family of Liliaceae, colourless and high-water content (99%) gel. [7-8].

2. EXPERIMENTAL

Self-Ignite green combustion method was used to synthesize the red emitting $BaTiO_3$:Eu^{3+} (1-11 mol %) nanophosphor with varying concentration. Barium nitrate [Ba $(NO_3)_2$(99.9%)], Tetra butyl titanate [$Ti(C_4H_9O)_4$(99.9%)] and Europium nitrate [Eu $(NO_3)_3.5H_2O$ (99.9%] used as oxidizers and A.V. plant gel as a fuel. The metal nitrates and A.V.gel are dissolved in double distilled water and then mixed using magnetic stirrer for 25 min to get a clear solution. The resultant solution was kept in a pre-heated muffle furnace maintained at 400 ± 10 ^{o}C for the combustion process. During the combustion, the flame persists for ~ 1 min. After the completion of combustion process, the dish was then taken out of the furnace and the powder was calcined at 800 ^{o}C for 3h to obtain the required phase. The prepared samples were characterized for their nano regime and then optical studies were carried out along with their use in solid state applications.

IARJSET ISSN (O) 2393-8021, ISSN (P) 2394-1588

International Advanced Research Journal in Science, Engineering and Technology

Impact Factor 7.105 ⁜ Vol. 9, Issue 2, February 2022

DOI: 10.17148/IARJSET.2022.9285

2.1. Results and discussion

Fig.1 shows the PXRD patterns and W-H plots of $BaTiO_3:Eu^{3+}$ (1-11 mol %) nanophosphors. The intense and narrow single diffraction peaks of PXRD patterns confirms the formation of single phase.Debye – Scherrer's equation and Williamson and Hall method were employed to determine the average particle size.

$$D = \frac{0.9\lambda}{\beta \cos\theta} \quad \text{---------- (1)}$$

Where 'β'; the diffracted full width at half maximum (FWHM in radian) caused by the crystallites, 'λ'; the wavelength of X-ray (1.542 Å), 'θ'; the Bragg angle and k; is the constant depends on the grain shape (0.90). The value of D was found to be in the range 20-29 nm tabulated in Table.1. These broadening in the peaks usually coupled with size of the crystalline (D) or the strains within the sample or sometimes both [9]. Therefore, both crystallite size (D) and the micro strain present in the phosphor were calculated and summarized in Table.1 using Williamsons Hall (W-H) equation [10].

$$\frac{\beta \cos\theta}{\lambda} = \frac{1}{D} + \frac{\varepsilon \sin\theta}{\lambda} \quad \text{..... (2)}$$

Table 1: Estimated crystallite size and strain values of $BaTiO_3:Eu^{3+}$ (1-11 mol %) nanophosphor.

$BaTiO_3:Eu^{3+}$ (mol %)	**Crystallite size (nm) [D-S approach]**	**Crystallite size(nm) [W-H approach]**	**Strain (x 10^{-4})**
1	20	21	1.6
3	28	23	1.7
5	24	28	1.2
7	29	24	1.5
9	26	27	1.6
11	25	25	1.7

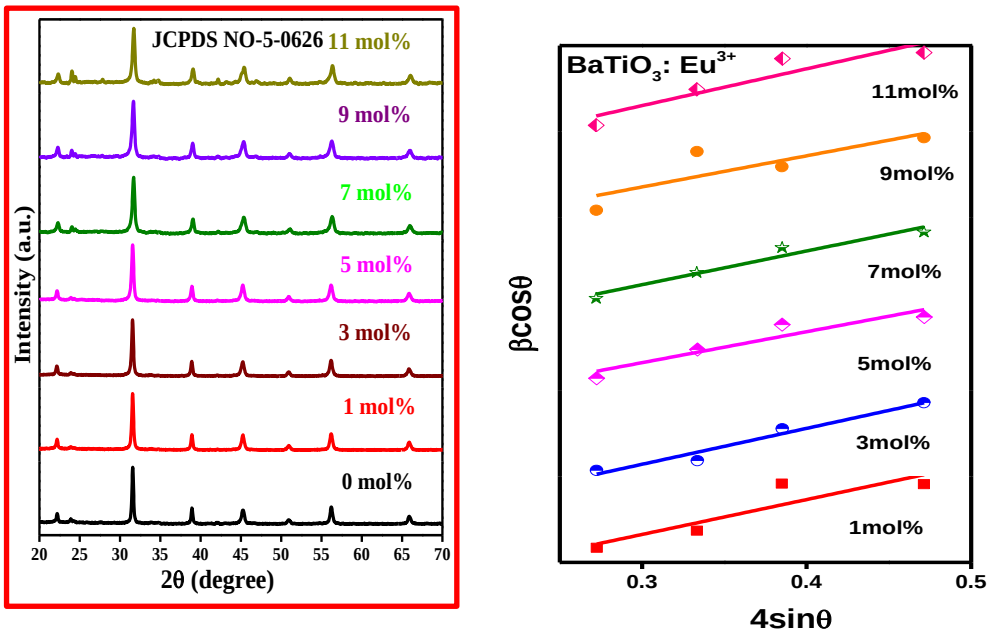

Fig. 1 PXRD patterns and W–H plots of $BaTiO_3$: Eu^{3+} (1–11 mol %) nanophosphors.

Fig.2 (a, b) shows the surface morphology of 5 mol % Eu^{3+} doped $BaTiO_3$ nanophosphor studied using SEM. It was clearly observed that, phosphor containing spherical shaped agglomerated particles having various sizes. The SEM images confirm that both the A.V. gel content and the concentration of Eu^{3+} were affecting the morphology of the samples.

The structural information of the $BaTiO_3:Eu^{3+}$(5 mol %) NPs were further investigated by TEM, HRTEM shown in Fig.3 (a,b).It was evident from the Fig.3(a) that, the particles were agglomerated in nature with average particle size was found to be in the range of 25 – 30 nm. Fig.3 (b) shows HRTEM with d-spacing was found to be 0.2981 nm. These results were in good agreement with the Scherer's and W-H plots.

IARJSET ISSN (O) 2393-8021, ISSN (P) 2394-1588

International Advanced Research Journal in Science, Engineering and Technology

Impact Factor 7.105 ⁜ Vol. 9, Issue 2, February 2022

DOI: 10.17148/IARJSET.2022.9285

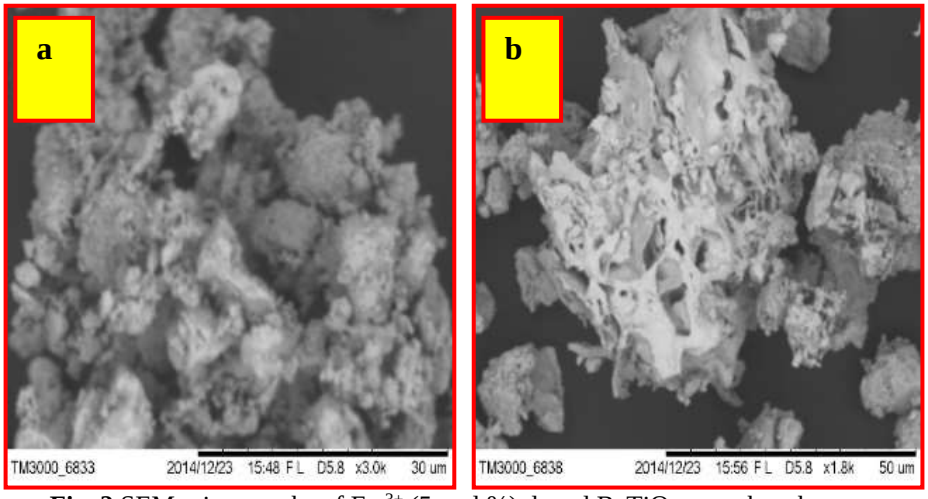

Fig. 2 SEM micrographs of Eu^{3+} (5 mol %) doped $BaTiO_3$ nanophosphors.

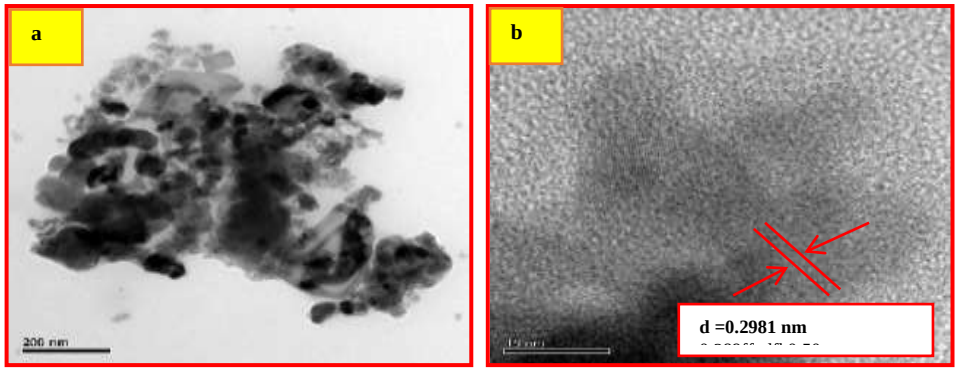

Fig. 3 TEM **(a)** and **(b)** HRTEM of $BaTiO_3$: Eu^{3+} (5 mol %) NPs

Fig.2 (a, b) shows the surface morphology of pure polypyrrole. It was clearly observed that, polypyrrole containing irregular shaped agglomerated particles having various sizes.

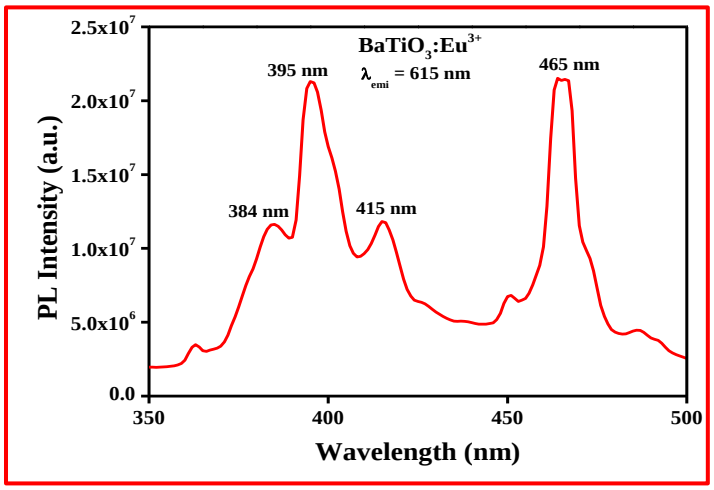

Fig.4.a PL excitation spectrum.

Fig.4. (a) shows the excitation spectrum of $BaTiO_3$:Eu^{3+} monitored at 615 nm emission was recorded in the range of 350-500 nm. The spectrum consists of intra peaks at 395 and 465 nm

and which were attributed to the configuration (f–f) transitions of Eu^{3+} ion. A series of excitation peaks at 395, 465 were mainly attributed to $^7F_0 \rightarrow {}^5G_5$, $^7F_0 \rightarrow {}^5D_2$ absorbing transition of 4f electrons of Eu^{3+} ion. The $BaTiO_3$: Eu^{3+} can be

IARJSET ISSN (O) 2393-8021, ISSN (P) 2394-1588

International Advanced Research Journal in Science, Engineering and Technology

Impact Factor 7.105 ⁜ Vol. 9, Issue 2, February 2022

DOI: 10.17148/IARJSET.2022.9285

strongly excited by near UV and blue light region; therefore, the present phosphor can be used as potential candidate for phosphor converted near UV-LED in solid state lightning.

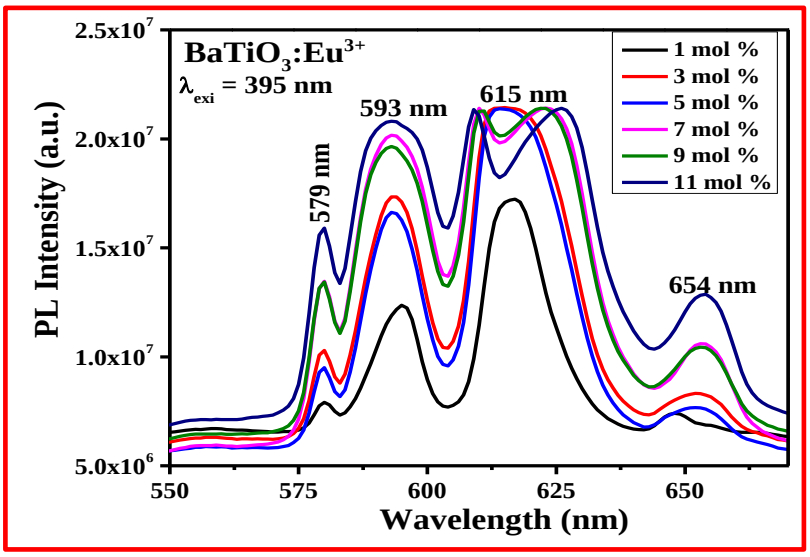

Fig.4.b Emission spectra of $BaTiO_3:Eu^{3+}$(1-11 mol %).

Fig.4. (b) shows the PL emission spectra excited at 395 nm. According to the energy level positions of Eu^{3+}ions, the emission peaks observed around 580, 593, 615 and 654 nm were attributed to the $^5D_0 \rightarrow {}^7F_0$, $^5D_0 \rightarrow {}^7F_1$, $^5D_0 \rightarrow {}^7F_2$ and $^5D_0 \rightarrow {}^7F_3$ transitions respectively]. In emission spectra, the peaks were narrow in nature due to electron shielding effect in rare-earth ions (Eu^{3+}). The peak at 615nm was electric –dipole transition $^5D_0 \rightarrow {}^7F_2$ which was much intense and hypersensitive in the host matrix [8-13]. It was observed that maximum emission intensity of $BaTiO_3:Eu^{3+}$phosphor appears at 5 mol %. The weak emission peak at 593nm was attributed to $^5D_0 \rightarrow {}^7F_1$ transition and ascribed to magnetic dipole transition which was insensitive to site symmetry. In the present case, dominance of $^5D_0 \rightarrow {}^7F_2$ transition specify that the location of Eu^{3+} ions diverge from the inversion symmetry, i.e., at low symmetry positions which can give the structural information of Eu^{3+} ions in the $BaTiO_3$ host matrix. At higher concentration, the luminescence intensity reduces contrarily owing to concentration quenching effect due to the energy transfer from one activator to the neighbouring ions. The PL intensity increased with increase of concentration of Eu^{3+} up to 5 mol % and afterwards it decreases. The decrease in PL intensity was due to phenomena known as self-quenching concentration of Eu^{3+} ions into the host matrix. When the phosphor was excited, the loss of absorbed energy by non-radiative energy transfer may be created large vacancies by incorporation of Eu^{3+} in $BaTiO_3$ host or Eu^{3+} - Eu^{3+} interactions. The non-radiative energy transfer between Eu^{3+} was mainly due to exchange interaction, radiation reabsorption, or a multipole–multipole interaction [14]

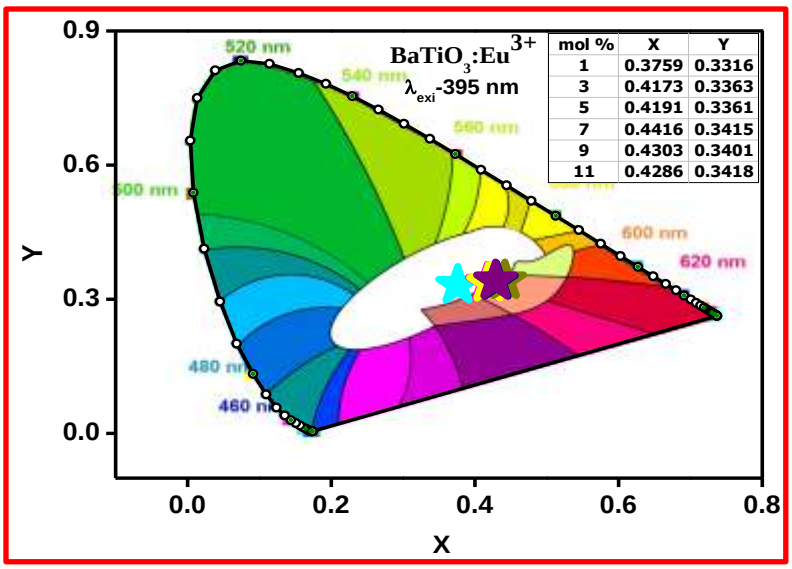

Fig.5 (a) CIE Chromaticity diagram of $BaTiO_3:Eu^{3+}$ (1-11 mol %)

IARJSET ISSN (O) 2393-8021, ISSN (P) 2394-1588

International Advanced Research Journal in Science, Engineering and Technology

Impact Factor 7.105 ⁜ Vol. 9, Issue 2, February 2022

DOI: 10.17148/IARJSET.2022.9285

The emission color of $BaTiO_3:Eu^{3+}$nanophosphors were investigated by using the 1931 CIE (Commission Internationale de L'Eclairage) system [15]. The CIE coordinates of $BaTiO_3:Eu^{3+}$located in red region **Fig.5 (a**).

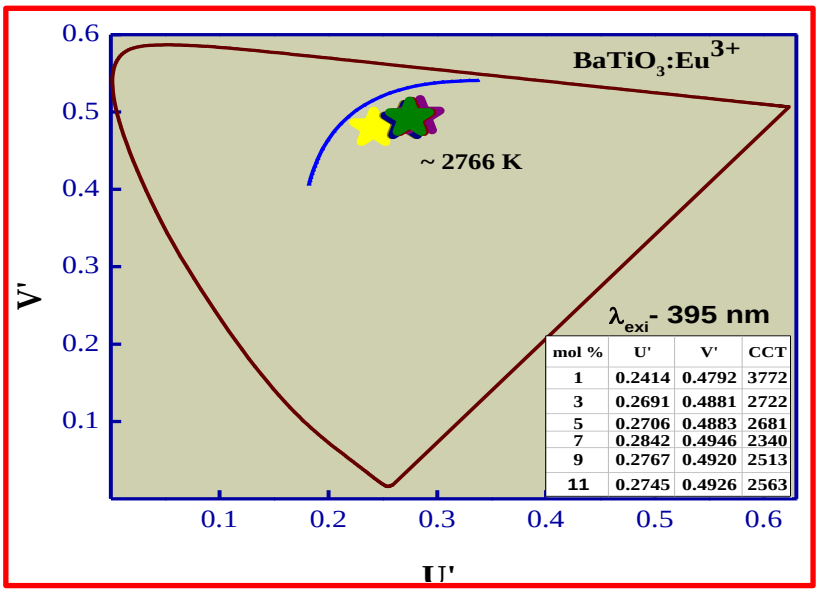

Fig.5 (b) CCT diagram

Further, the calculated average CCT value of nanophosphors were found to be in the range of 2340-2766 K which was within the range of vertical daylight **Fig.5 (b**). The results revealed that the phosphor is quite useful candidate for display applications. The CCT rating for a lamp or a source is a general ''warmth'' or ''coolness'' measure of its appearance. However, opposite to the temperature scale, lamps with a CCT rating below 3200 K was commonly considered as ''warm'' sources, whereas those with a CCT above 4000 K was generally considered ''cool'' in appearance [16]. Correlated Color Temperature (CCT) can be estimated by Planckian locus, which was only a small portion of the (x, y) chromaticity diagram and there exist many operating points outside the Planckian locus. If the coordinates of a light source do not fall on the Planckian locus, the coordinated color temperature (CCT) was used to define the color temperature of a light source.

2.2. CONCLUSIONS:

$BaTiO_3:Eu^{3+}$(1-11 mol %) nanophosphors were synthesized by a solution combustion method using Aloe Vera gel as fuel. The diffraction patterns of the nanophosphors were indexed to tetragonal phase with average crystallite size in the range 25-30 nm. The emission peaks ascribed to $^5D_0 \rightarrow {}^7F_0$,$^5D_0 \rightarrow {}^7F_1$,$^5D_0 \rightarrow {}^7F_2$ and $^5D_0 \rightarrow {}^7F_3$. Based on CIE and CCT coordinates, the phosphor materials can be a good candidate for the display device applications. The rare earth doped luminescent titanates phosphors are considered to be probable candidates as fluorescent labelling markers for enhanced detection of latent fingerprints on variety of substances.

REFERENCES:

[1]. C. Guo, S. Wang, T. Chen, L. Luan, Y. Xu, Appl. Phys., A 94 (2009) 365-371
[2]. E.F. Schubert, J.K. Kim, Science, 308 (2005) 1274–1278.
[3]. Santosh K. Gupta, V. Grover, R. Shukla, K. Srinivasu, V. Natarajan, A.K. Tyagi, Chem. Eng., 283 (2016) 114–126
[4]. P.K. Dutta, R. Asiaie, S.A. Akbar, W.D. Zhug, Chem. Mater., 6 (1994) 1542–1548.
[5]. X.R. Xing, J.X. Deng, J. Chen, G.R. Liu, J. Alloys Comp., 384 (2004) 312–317.
[6]. Y.L. Wang, X.L. Chen, H.F. Zhou, L. Fang, L.J. Liu, H. Zhang, J. Alloys Comp. 551(2014) 365–369.
[7]. S.P. Dubey, M. Lahtinen, M. Sillanpa, Colloids Surf. A 364 (2010) 34- 41.
[8]. S.F.Wang, F. Gu,M.K. Lu, Z.S. Yang, G.J. Zhou,H.P. Zhang, Y.Y. Zhou, S.M.Wang,Opt. Mater.28 (2006) 1222–1226.
[9]. B. D. Cullity, Elements of X-ray diffraction, Addison Wesley, 1978.
[10]. G.P. Darshan, H.B. Premkumar, H. Nagabhushana, S.C. Sharma, S.C. Prashanth, B. Daruka Prasad, J. Colloids and Interface Sci.464(2016) 206-218.

IARJSET ISSN (O) 2393-8021, ISSN (P) 2394-1588

International Advanced Research Journal in Science, Engineering and Technology

Impact Factor 7.105 ⁜ Vol. 9, Issue 2, February 2022

DOI: 10.17148/IARJSET.2022.9285

[11]. S. Som, A. K. Kunti, Vinod Kumar, Vijay Kumar, S. Dutta, M. Chowdhury, S. K. Sharma, J. J. Terblans, H. C.Swart, Journal of Applied Physics **115**, 193101 (2014).
[12]. LI Mengting, JIAO Baoxiang, Journal of Rare Earths**,** Vol. 33, No. 3, Mar. 2015, P. 231.
[13]. J. P. Rainhoa, D. Ananias, Z. Lin, A. Ferreira, L. D. Carlos, and J. Rocha, J. Alloys Compd. 374, 185 (2004).
[14]. D. L. Dexter, J. Chem. Phys. 21 (1953) 836-850.
[15]. Publication CIE no 17.4 (1987) International Lighting Vocabulary, Central Bureau of the Commission Internationale de L 'Eclairage, Vienna, Austria
[16]. JánosSchanda, M Danyi, "Correlated Color-Temperature Calculations in the CIE 1976 Chromaticity Diagram", Color Res. Appl., 2 (1977) 161-163.